Ground- and Excited-State Reactions of Norbornene and Isomers: A CASSCF Study and Comparison with Femtosecond Experiments

**Sarah Wilsey,[†] K. N. Houk,*,[†] and A. H. Zewail[‡]**

Contribution from the Department of Chemistry and Biochemistry, University of California, Los Angeles, California 90095-1569, and Arthur Amos Noyes Laboratory of Chemical Physics, California Institute of Technology, Pasadena, California 91125

Abstract: The ground-state and $^1(\pi\pi^*)$-state potential energy surfaces of norbornene and isomeric C_7H_{10} species were mapped using CASSCF theory and the 6-31G* basis set and compared with the results of femtosecond experiments on norbornene retro Diels−Alder reactions. Computations explored stepwise and concerted retro Diels−Alder pathways, [1,3]-sigmatropic shifts, and [1,2]-sigmatropic shifts originating from the $^1(\pi\pi^*)$-state or ground-state surfaces. Extremely efficient decay occurs from the excited state to the ground state via two different conical intersections (surface crossings). The first of these crossing points is accessed by one-bond cleavage of C1−C6 (or C4−C5). Several possible subsequent ground-state reaction paths have been identified: (a) ring-closure to form norbornene; (b) ring-closure to form bicyclo[3.2.0]hept-2-ene ([1,3]-sigmatropic shift); (c) formation of a metastable 1,3-biradical which closes to form tricyclo[3.2.1.0^{3,7}]heptane ([1,2]-sigmatropic shift); and (d) collapse of a *gauche-in* biradical to a vibrationally excited cyclopentadiene and ethylene, or norbornene. Excited-state one-bond cleavage of C4−C7 (or C1−C7) leads to the second conical intersection. Possible ground-state reaction pathways from this structure lead to the formation of bicyclo-[4.1.0]hept-2-ene ([1,3]-sigmatropic shift product) or to a second 1,3-biradical leading to tricyclo[3.2.1.0^{3,7}]-heptane ([1,2]-sigmatropic shift product). The vibrationally excited cyclopentadiene is the 220 fs lifetime species of mass 66 amu, consistent with the retro Diels−Alder reaction observed in the femtosecond laser experiments. It is proposed that biradicaloids formed after decay through the conical intersections are the 94 amu species, with an average lifetime of about 160 fs.

Introduction

Femtosecond-resolved spectroscopic detection of intermediates in a simple retro Diels−Alder reaction has created great excitement.[1] The thermal unimolecular dissociation of norbornene **1** into ethylene and cyclopentadiene is a classic example of a retro Diels−Alder reaction,[2] the mechanisms of which have caused much controversy.[3,4] Simple cases, lacking radical

1
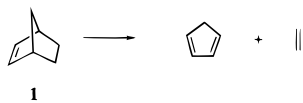
stabilizing groups, are generally believed to occur via concerted mechanisms in which the two bonds in the transition state are broken simultaneously. The competing stepwise processes via biradical intermediates lie several kilocalories per mole higher in energy. For norbornene, the computed difference is a substantial 12 kcal/mol,[5] consistent with the stereospecificity of reactions of deuterium-labeled cases.

Zewail and co-workers recently communicated femtosecond experiments which raised the possibility that the lifetime of a biradical intermediate formed in a stepwise process was too short for rotation about single bonds to occur; experimental stereospecificity might be observed even with a stepwise mechanism.[1] The reaction was followed using femtosecond-resolved laser energization and detection, aided by mass spectrometric detection of transient masses. The buildup and decay of two different short-lived species were observed during the reaction, one with the mass of norbornene ($\tau = 160$ fs) and one with the mass of cyclopentadiene ($\tau = 220$ fs). To be detected, these species need to be easily ionized, and are therefore not ground-state species. The buildup of the second species did not correlate with the decay of the first, suggesting that two different reaction paths are populated. Zewail and co-workers suggested that the norbornene species is a biradical formed in a stepwise retro Diels−Alder process, while the second species is cyclopentadiene in either a vibrationally or electronically (possibly Rydberg) excited state, formed in a concerted process.[1]

[†] University of California, Los Angeles.

[‡] California Institute of Technology.

(1) Horn, B. A.; Herek, J. L.; Zewail, A. H. *J. Am. Chem. Soc.* **1996**, *118*, 8755−8756.

(2) (a) Diels, O.; Alder, K. *Justus Liebigs Ann. Chem.* **1928**, *460*, 98. (b) Diels, O.; Alder, K. *Ber. Dtsch. Chem. Ges. A* **1929**, *62*, 554.

(3) Dewar, M. J. S.; Jie, C. *Acc. Chem. Res.* **1992**, *22*, 537−543.

(4) (a) Houk, K. N.; Gonzalez, J.; Li, Y. *Acc. Chem. Res.* **1995**, *28*, 81−90. (b) Borden, W. T.; Loncharich, E. J.; Houk, K. N. *Annu. Rev. Phys. Chem.* **1988**, *39*, 213. (c) Houk, K. N.; Li, Y.; Evanseck, J. D. *Angew. Chem., Int. Ed. Engl.* **1992**, *31*, 682.

(5) Beno, B. R.; Wilsey, S.; Houk, K. N. *J. Am. Chem. Soc.*, in press. See also: Tian, J.; Houk, K. N.; Klärner, F.-G.; *J. Phys. Chem.* **1998**, *102*, 7662−7667.

(6) (a) Baldwin, J. E.; Belfield, K. D. *J. Am. Chem. Soc.* **1988**, *110*, 296. (b) Klärner, F.-G.; Drewes, R.; Hasselman, D. *J. Am. Chem. Soc.* **1988**, *110*, 297.

(7) (a) Berson, J. A.; Holder, R. W. *J. Am. Chem. Soc.* **1973**, *95*, 2037. (b) Berson, J. A.; Salem, L. *J. Am. Chem. Soc.* **1972**, *94*, 8917. (c) Berson, J. A. *Acc. Chem. Res.* **1972**, *5*, 406. (d) Berson, J. A.; Nelson, G. L. *J. Am. Chem. Soc.* **1970**, *92*, 1096. (e) Berson, J. A.; Nelson, G. L. *J. Am. Chem. Soc.* **1967**, *89*, 5503. (f) Newman-Evans, R. H.; Carpenter, B. K. *J. Am. Chem. Soc.* **1984**, *106*, 7994.

Inspired by these experiments, we have recently completed a thorough mapping of the ground-state surface of norbornene using density functional theory (DFT) with the B3LYP functional and the 6-31G* set.[5] Both the retro Diels−Alder reaction of norbornene and the ground-state isomerization of bicyclo-[3.2.0]hept-2-ene **2** to form norbornene were examined. The


2
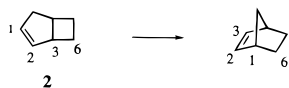
latter has been studied experimentally[6,7] and with trajectory calculations on a semiempirical potential surface.[8] The Woodward−Hoffmann [1*i*,3*s*] stereochemistry[9] is usually favored in such reactions, even though biradical intermediates are thought to be formed.[6−8] The DFT calculations show that there is no stable intermediate formed in this process.[5] An extremely flat biradical region on the potential surface leads to closure to norbornene with inversion of stereochemistry, while competing closure with retention of stereochemistry has an additional barrier of about 1 kcal/mol.

To compare the results of the femtosecond experiments with theoretical calculations, it is imperative to study not only the ground state surface but the surface topology of the excited state surface as well. The buildup of both intermediates detected experimentally is extremely fast: the buildup of the species with mass 94 amu occurs with the rise of the laser pulse, while the species with mass 66 amu builds up in about 30 fs. This suggests that there must be a mechanism whereby extremely efficient decay takes place from the excited-state to the ground-state surface. This, in turn, implies the presence of a conical intersection, such as the one recently reported by Robb and co-workers in the photocycloaddition of ethene to benzene.[10] Decay through such a feature is known to be exceedingly fast and normally occurs within a single vibrational period of the molecule.[11] As we will describe later, these crossing points also play a fundamental role in the photochemistry of norbornene.

The species with a lifetime of 220 fs and the mass of cyclopentadiene has been identified as a vibrationally excited cyclopentadiene, although it is also conceivably a Rydberg state of cyclopentadiene. Two distinct 3p Rydberg states of cyclopentadiene have been identified experimentally in the 195-nm region, with lifetimes greater than 130 fs.[12]

The 3s Rydberg state of norbornene is known to lie lower in energy than the valence $\pi\pi^*$ state.[13,14] However, this state is generally believed to give rise to carbene products, leading to 1,2 H-shifts or 1,2 C-shifts, and not to retro Diels−Alder products.[13] Rearrangements from the $^1(\pi\pi^*)$ state of norbornenes are known for 2-cyanonorbornene[15a] and 2-trifluoromethyl-2-norbornene.[15b] In both of these, the $^1(\pi\pi^*)$ state lies below the Rydberg (π,3s) state. On direct irradiation of 2-cyanonorbornene,

3b and **4b** were formed in a 20:1 ratio. Cleavage of the C4−

a: R=H
b: R=CN
c: R=CF$_3$
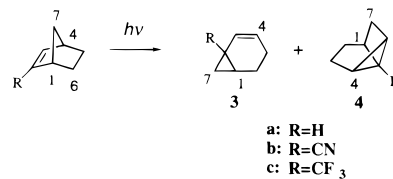
C7 bond can lead to a [1,3]-sigmatropic shift to give **3b**, or a [1,2]-sigmatropic shift to give **4b**. Alternatively, initial cleavage of the C1−C6 bond, followed by a [1,2]-sigmatropic shift, could give **4b**. Photolysis of 2-trifluoromethyl-2-norbornene in solution gave mainly **3c**.

We have investigated $^1(\pi\pi^*)$ excited-state reaction pathways for norbornene to provide a more detailed picture of the dynamics. The triplet $\pi\pi^*$ surface of norbornene has been investigated previously using CASSCF, MRD-CI, and unrestricted DFT methods.[16] The singlet $\pi\pi^*$ surface is significantly different. Conical intersection regions on the potential surface where decay to the ground-state surface can occur have been located, and ground-state reaction paths leading from these conical intersections to a variety of products have been identified.

This paper first describes the results obtained in the Zewail experiments, then describes the computational studies of the C_7H_{10} excited- and ground-state surfaces, and finally provides a comparison with the femtosecond experiments.

Experimental Details

The experiments at Caltech involved preparation of the excited-state species by two-photon absorption from a 310-nm femtosecond laser pulse. This delivers 184 kcal/mol (8.0 eV) of energy, well above the energy of both the lowest singlet excited valence ($\pi\pi^*$) and the Rydberg states of norbornene, which have experimental energies of 146 and 137 kcal/mol, respectively.[14]

The femtosecond transients were obtained by mass gating the time-of-flight mass spectrometer and sweeping the time delay. The mass spectrum of norbornene obtained in the gas phase after the laser pulse shows only two peaks, as mentioned above: one at mass 94 amu, which is the mass of norbornene, and a second at mass 66 amu, which is the mass of cyclopentadiene. These observations are consistent with retro Diels−Alder products found in thermal,[17] photochemical,[18] and shock wave[19] studies.

The 94-amu signal intensity rises with the response function of the laser pulse and decays exponentially back to its original intensity level with a decay time, τ, of 160 ± 15 fs. On the other hand, the signal from the 66-amu fragment rises very rapidly and decays exponentially back to near the original intensity level. Fitting this to a rise and decay biexponential function gave a rise time of $\tau_1 = 30 \pm 5$ fs and a decay time of $\tau_2 = 220 \pm 20$ fs. When the energy in norbornene was varied to 137 kcal/mol, the values $\tau = 175$, $\tau_1 = 40$, and $\tau_2 = 200$ fs were obtained.

The femtosecond results indicate that, on this time scale, there exists an excited product with mass 66 amu, corresponding to the rapid cleavage of two bonds. It is also evident that an intermediate with mass 94 amu is formed which disappears in 160 fs. The magnitudes of the lifetimes of these species are reminiscent of those observed for

(8) (a) Carpenter, B. *J. Am. Chem. Soc.* **1996**, *118*, 10329. (b) Carpenter, B. *J. Am. Chem. Soc.* **1995**, *117*, 6336.

(9) Woodward, R. B.; Hoffmann, R. *The Conservation of Orbital Symmetry*; Verlag Chemie: Weinheim, 1970.

(10) Clifford, S.; Bearpark, M. J.; Bernardi, F.; Olivucci, M.; Robb, M. A.; Smith, B. R. *J. Am. Chem. Soc.* **1996**, *118*, 7353.

(11) (a) Zimmerman, H. E. *J. Am. Chem. Soc.* **1966**, *88*, 1566. (b) Michl, J. *J. Mol. Photochem.* **1972**, 243. (c) Teller, E. *Isr. J. Chem.* **1969**, *7*, 227.

(12) McDiarmid, R.; Sabljic, A. *J. Phys. Chem.* **1991**, *95*, 6455.

(13) (a) Srinivasan, R.; Brown, K. H. *J. Am. Chem. Soc.* **1978**, *100*, 4602. (b) Inoue, Y.; Mukai, T.; Hakushi, T. *Chem. Lett.* **1982**, 1045.

(14) Stokes, S.; Pickett, L. W. *J. Chem. Phys.* **1955**, *23*, 258. (b) Wen, A. T.; Hitchcock, A. P.; Werstiuk, N. H.; Nguyen, N.; Leigh, W. J. *Can. J. Chem.* **1990**, *68*, 1967.

(15) (a) Akhtar, I. A.; McCullough, J. J.; Vaitekunas, S. *Can. J. Chem.* **1982**, *60*, 1658. (b) Nguyen, N.; Harris, B. E.; Clark, K. B.; Leigh, W. J. *Can. J. Chem.* **1990**, *68*, 1961.

(16) Grimme, S.; Woeller, M.; Peyerimhoff, S. D.; Danovich, D.; Shaik, S. *Chem. Phys. Lett.* **1998**, *287*, 601.

(17) (a) Herndon, W. C.; Cooper, W. B.; Chambers, M. J. *J. Phys. Chem.* **1964**, *68*, 2016. (b) Roquitte, B. C. *J. Phys. Chem.* **1965**, *69*, 1351. (c) Salazar, J.; Marquez, M.; Barriola, A. *Acta Cient. Venez.* **1987**, *38*, 505. (d) Woods, W. G. *J. Org. Chem.* **1958**, *23*, 110. (e) Birely, J. H.; Chesick, J. P. *J. Phys. Chem.* **1962**, *66*, 568.

(18) Roquitte, B. C. *J. Phys. Chem.* **1965**, *69*, 2475.

(19) (a) Kiefer, J. H.; Kumaran, S. S.; Sundaram, S. *J. Chem. Phys.* **1993**, *99*, 3531. (b) Barker, J. R.; King, K. D. *J. Chem. Phys.* **1995**, *103*, 4953.

trimethylene ($<$120 fs),[20] tetramethylene (700 fs),[20] and acetyl intermediates (500−750 fs at 307 nm; 180−280 fs at 280 nm).[21]

Computational Methods

All energies were computed using CASSCF theory and the 6-31G* basis set in GAUSSIAN 94.[22] An active space comprising eight electrons in eight orbitals (π, π^*, σ, σ^* in the C2=C3 bond and the σ, σ^* orbitals in the C1−C6 and C4−C5 bonds that are broken) was used for the reaction paths involving initial C1−C6 bond cleavage (retro Diels−Alder, [1,3]-sigmatropic shift to form **2**, and [1,2]-sigmatropic shift to form **4a**). A smaller active space of six electrons in six orbitals was used for the reaction paths involving initial C4−C7 bond cleavage. This included the π, π^*, σ, and σ^* orbitals in the C2=C3 bond and the σ and σ^* orbitals in the C4−C7 bond. In both cases, the C2=C3 σ and σ^* orbitals were included because of the proximity of the $^1(\pi\pi^*)$ and $^1(\sigma\pi^*)$ states in the region of the reactant.

The conical intersection structures were located using the algorithm in GAUSSIAN 94 which optimizes the lowest energy point on an $n - 2$ crossing seam (n is the number of degrees of freedom in the molecule), where two surfaces are degenerate.[23] The remaining two coordinates are a linear combination of the gradient difference vector,

$$\frac{\partial(E_0 - E_1)}{\partial q}$$

and the derivative coupling (or nonadiabatic coupling) vector,

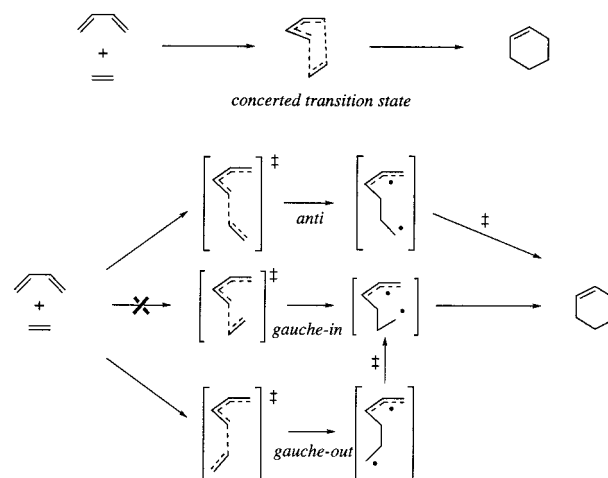$$\left\langle \Psi_0 \left| \frac{\partial \Psi_1}{\partial q} \right\rangle \right.$$

which are obtained during the optimization procedure, where q refers to the nuclear coordinates, E_m refers to the energy of the mth state, and Ψ_m is the corresponding wave function. The first of these defines the direction in which the difference between the gradients of the two surfaces is largest, while the second couples the electronic and vibrational motions of the two states, which is necessary as the Born−Oppenheimer approximation does not hold in such regions.

The $(n - 2)$-dimensional conical intersection hyperline is infinitely long, but normally it is assumed that most of the molecules decay in the region around the lowest energy point on this hyperline. At such a point, the gradients are zero along all coordinates except the gradient difference and derivative coupling vectors, such that a molecule starting from this point with zero momentum would follow reaction paths defined by these vectors. It is, therefore, normally assumed that most of the molecules decaying through the conical intersection will follow these vectors on the lower energy surface after decay, unless there is a large amount of momentum in a direction orthogonal to them.[23b]
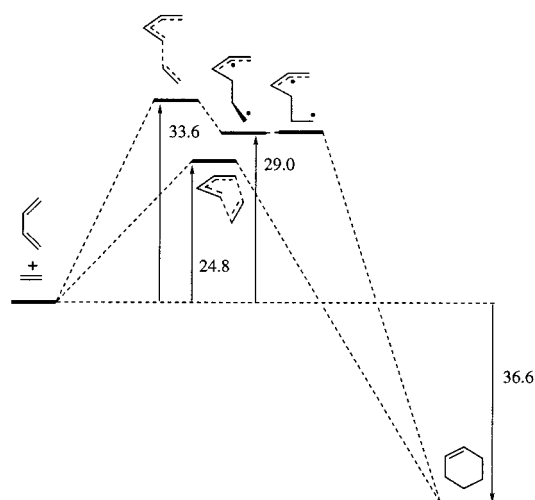
The product distribution depends on the reaction paths taken, which in turn will depend on the direction which the molecule approaches the conical intersection (see ref 10). It is possible to predict product distributions using molecular dynamics, but without dynamics calculations it is very difficult to predict a favored pathway.

Conical intersections and neighboring structures were optimized using state-averaged orbitals. Transition states were optimized using

(20) Pederson, S.; Herek, J. L.; Zewail, A. H. *Science* **1994**, *266*, 1359.

(21) Kim, S. K.; Pedersen, S.; Zewail, A. H. *J. Chem. Phys.* **1995**, *103*, 477.

(22) Frisch, M. J.; Trucks, G. W.; Schlegel, H. B.; Gill, P. M. W.; Johnson, B. G.; Robb, M. A.; Cheeseman, J. R.; Keith, T. A.; Petersson, G. A.; Montgomery, J. A.; Raghavachari, K.; Al-Laham, M. A.; Zakrzewski, V. G.; Ortiz, J. V.; Foresman, J. B.; Cioslowski, J.; Stefanov, B. B.; Nanayakkara, A.; Challacombe, M.; Peng, C. Y.; Ayala, P. Y.; Chen, W.; Wong, M. W.; Andres, J. L.; Replogle, E. S.; Gomperts, R.; Martin, R. L.; Fox, D. J.; Binkley, J. S.; Defrees, D. J.; Baker, J.; Stewart, J. P.; Head-Gordon, M.; Gonzalez, C.; Pople, J. A. *GAUSSIAN 94 (Revision B2)*; Gaussian, Inc.: Pittsburgh, PA, 1995.

(23) (a) Bearpark, M. J.; Robb, M. A.; Schlegel, H. B. *Chem. Phys. Lett.* **1994**, *223*, 269. (b) Olivucci, M.; Bernardi, F.; Celani, P.; Ragazos, I.; Robb, M. A. *J. Am. Chem. Soc.* **1994**, *116*, 1077. (c) Klessinger, M. *Angew. Chem., Int. Ed. Engl.* **1995**, *34*, 549.

Scheme 1

Scheme 2

an initial guess for the Hessian generated using the redundant coordinate code. Frequencies proved too expensive to compute with the (8,8) active space and were, therefore, computed in a reduced active space of four electrons in four orbitals to check the nature of the critical point located. CASPT2N energies were computed using the method of Roos et al.[24] as implemented in MOLCAS.[25]

Results and Discussion

Ground-State Surface. We first describe the CASSCF/6-31G* ground-state surface topology and compare it with the results we previously obtained at the UB3LYP/6-31G* level.[5] The geometries obtained at the CASSCF/6-31G* level are shown in Figures 1−13, and the energies obtained using both methods are given in Tables 1−4. The UB3LYP results for the ground state provide better agreement with experiment than the CASSCF results, which are known to lack some dynamic correlation and have a tendency to favor biradical species. Therefore, in the following discussion of the ground-state surface, the energies given are those obtained at the UB3LYP level where known, followed by the CASSCF values in parentheses.

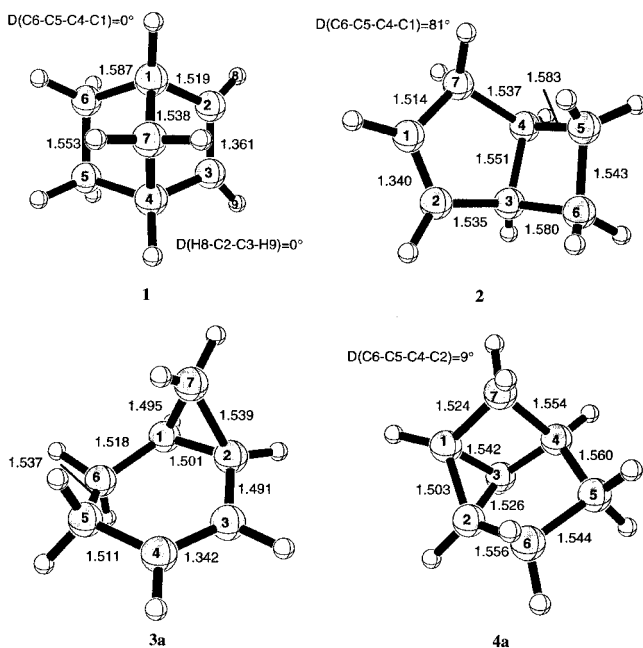(24) Andersson, K.; Malmqvist, P.-Å.; Roos, B. O. *J. Chem. Phys.* **1992**, *96*, 1218.

(25) Andersson, K.; Blomberg, M. R. A.; Fülscher, M. P.; Kellö, V.; Lindh, R.; Malmqvist, P.-Å.; Noga, J.; Olson, J.; Roos, B. O.; Sadlej, A. J.; Siegbahn, P. E. M.; Urban, M.; Widmark, P.-O. *MOLCAS (version 2.0)*; University of Lund, Sweden, 1991.

Figure 1. CASSCF/6-31G*-optimized geometries of norbornene **1**, bicyclo[3.2.0]hept-2-ene **2**, bicyclo[4.1.0]hept-2-ene **3a**, and tricyclo-[3.2.1.0³,⁷]heptane **4a**.

(i) Retro Diels−Alder Pathway of Norbornene To Form Cyclopentadiene and Ethylene. The UB3LYP/6-31G* computed ground-state surface of the parent Diels−Alder reaction of ethylene and *s-cis*-butadiene was examined earlier by Goldstein, Beno, and Houk.[26] Both concerted and stepwise pathways of the type shown in Scheme 1 were computed. A sketch of the reaction profile obtained, showing the energies of stationary points, is given in Scheme 2. The concerted path is the lowest in energy by 9 kcal/mol and corresponds to the synchronous formation of the two new bonds. The lowest energy stepwise path proceeds through an *anti* transition state to an *anti* biradical intermediate. Closure to cyclohexene involves predominantly torsion about the first bond formed. However, a transition state for this process could not be located since the surface is so flat with respect to this motion. An alternative stepwise path proceeds through a *gauche-out* transition structure, which lies 2 kcal/mol higher in energy than the corresponding *anti* structure. The third possible biradical conformer would be the *gauche-in* biradical; however, this species is unstable to C−C bond formation and could not be located. Ring-closure from the *gauche-out* biradical is expected to proceed through this nonstationary *gauche-in* species. CASSCF studies of this reaction gave qualitatively similar results.[27]

The energies of the critical points located along the ground-state reaction path for the retro Diels−Alder reaction of norbornene **1** (Figure 1) to form cyclopentadiene and ethylene using UB3LYP/6-31G* and CASSCF/6-31G* are given in Table 1. At both levels of theory, the reaction profile for the retro Diels−Alder reaction of norbornene is similar to that of the parent reaction (see Scheme 3). The barrier for the concerted reaction via the concerted transition state **5** (Figure 2) is 40.8 kcal/mol (51.3 kcal/mol), compared to 42.5 kcal/mol experimentally. The reaction is of the synchronous "aromatic" type,[4] with breaking C−C bond lengths of 2.22 Å and partial double bond lengths of 1.40−1.42 Å.

Along the lowest energy stepwise path, a transition state **6** between norbornene and an *anti* biradical **7** were located (Figure

(26) Goldstein, C.; Beno, B.; Houk, K. N. *J. Am. Chem. Soc.* **1996**, *118*, 6036.

**Table 1.** Energies along the Retro Diels−Alder Reaction Pathways at the UB3LYP/6-31G* and CASSCF(8,8)/6-31G* Levels

	E_{rel} (kcal/mol)[a]	
structure	UB3LYP/6-31G*[b]	CAS(8,8)/6-31G*
norbornene (**1**)	0.0	0.0
concerted TS (**5**)	40.8	51.3
anti TS1 (**6**)	53.2	58.4
anti biradical (**7**)	48.1	52.9
anti TS2 (**8**)	52.8	58.9
gauche-out TS1 (**9**)	53.0	58.2
gauche-out biradical (**10**)	48.3	53.0
gauche-out TS2 (**11**)	53.5	60.3
gauche-in biradical (**12**) inflection point	–	54.0[c]
ethylene + cyclopentadiene	18.4	12.9

[a] Energy relative to norbornene. [b] Energy includes ZPE correction. [c] Forces converged, but displacements not converged.
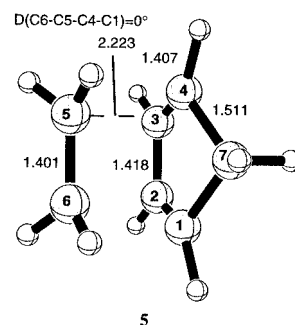
Figure 2. CASSCF/6-31G*-optimized geometry of the concerted Diels−Alder transition state **5**.

Scheme 3
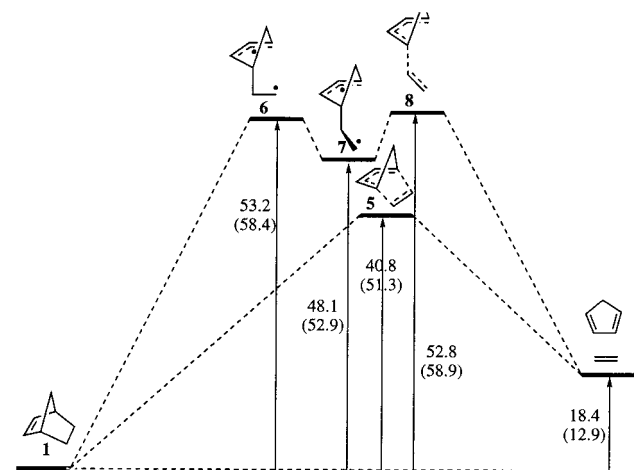
3). This transition state lies 12.4 kcal/mol (7.1 kcal/mol) above the concerted transition state and involves mainly torsion about the C4−C5 bond. The *anti* biradical lies 5.1 kcal/mol (5.5 kcal/mol) lower in energy and has a barrier to fragmentation via **8** of 4.7 kcal/mol (6.0 kcal/mol). The *gauche-out* stepwise pathway lies 0.3 kcal/mol (1.4 kcal/mol) above the *anti* stepwise pathway. Stationary points along this path (Figure 4) include the transition state **9** for forming the *gauche-out* biradical, the *gauche-out* biradical **10**, and the fragmentation barrier **11**.
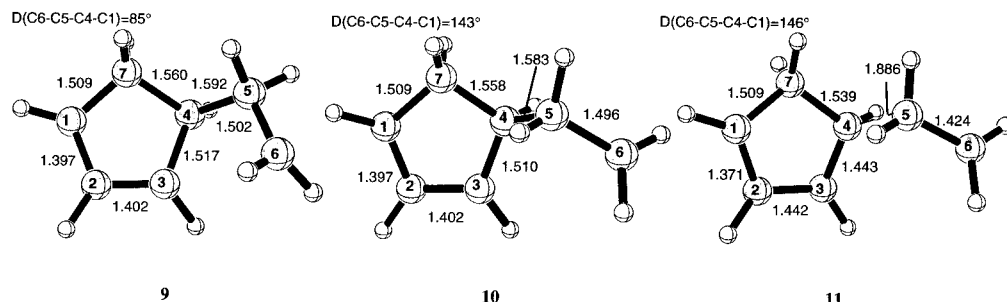
Both of the transition states (**6** and **9**) leading to the biradicals (**7** and **10**) correspond mainly to torsion about the C4−C5 bond. There is no maximum corresponding to simply stretching the C1−C6 bond and no stable minimum corresponding to a *gauche-in* biradical. Constrained optimizations were carried out

(27) Li, Y.; Houk, K. N. *J. Am. Chem. Soc.* **1993**, *115*, 7478.
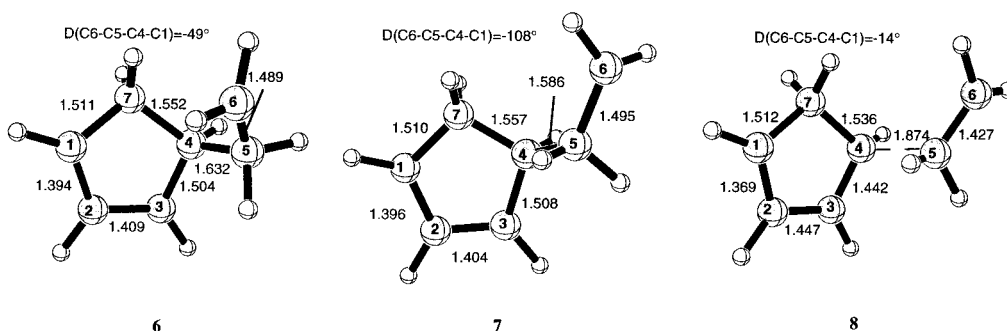
Figure 3. CASSCF/6-31G*-optimized geometries of the transition state leading to the *anti* biradical from norbornene **6**, the *anti* biradical **7**, and the transition state for *anti* biradical fragmentation **8** along a stepwise retro Diels−Alder pathway.
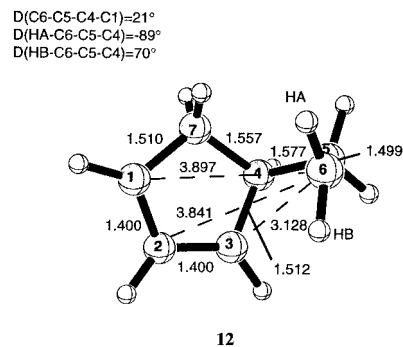

Figure 4. CASSCF/6-31G*-optimized geometries of the transition state leading to the *gauche-out* biradical from norbornene **9**, the *gauche-out* biradical **10**, and the transition state for *gauche-out* biradical fragmentation **11** along a stepwise retro Diels−Alder pathway.

Scheme 4
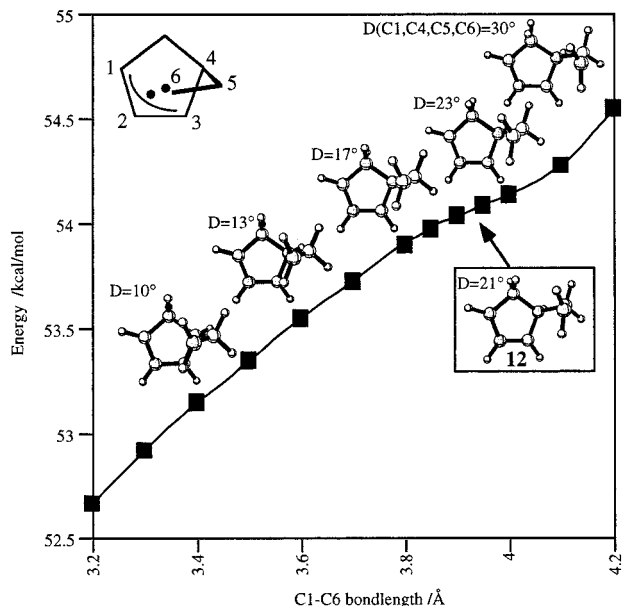
where the C1−C6 bond was kept fixed and all other parameters were optimized. This search (Scheme 4) clearly indicates that there is no distinct minimum corresponding to a stable *gauche-in* biradical species nor a transition state corresponding to cleavage of the C1−C6 bond, unless torsion, as in the *anti* or *gauche-out* transition states, occurs. The best structure (**12**) that could be optimized in this region (the forces are converged but the displacements are not) is shown in Figure 5. This structure has a small amount of rotation about the C4−C5 bond (21°), as well as pyramidalization of the radical center at C6, such that bonding to C1, C2, or C3 is minimized. This maximizes coupling with C4−C5, and no fragmentation barrier for cleaving the second bond in this species could be found. All attempts to find the transition state for cleavage led to the concerted transition state, as the geometries are similar and the concerted


Figure 5. CASSCF/6-31G*-optimized geometry of the metastable *gauche-in* biradical **12** (displacements not converged).

transition state lies considerably lower in energy. The *gauche-in* species **12** is essentially a distorted form of the concerted transition state, in the same vibrational energy basin on the potential surface.

(ii) [1,3]-Sigmatropic Shift of Norbornene To Form Bicyclo[3.2.0]hept-2-ene. Norbornene can undergo a second ground-state rearrangement to form bicyclo[3.2.0]hept-2-ene, **2** (Figure 1), although the reaction is energetically favored in the reverse direction. This is formally a [1,3]-sigmatropic shift, involving cleavage of the C1−C6 bond, accompanied by formation of the C3−C6 bond. Reaction paths leading from bicyclo[3.2.0]hept-2-ene to norbornene corresponding to both inversion and retention of stereochemistry at C6 have been identified. Scheme 5 shows all possible reaction paths connecting bicyclo[3.2.0]heptene to norbornene, where Newman projections down the C5−C6 bond are used to illustrate the various conformations of the critical points along these paths. Geometries along these reaction paths have also been optimized at the UB3LYP level,[5] and in Table 2 these results are compared to the results obtained at the CASSCF level.

Bicyclo[3.2.0]hept-2-ene lies 5.4 kcal/mol (9.5 kcal/mol) higher in energy than norbornene. Near the geometry of **2**, a transition state, **13** (Figure 6), corresponding to C3−C6 bond

Scheme 5
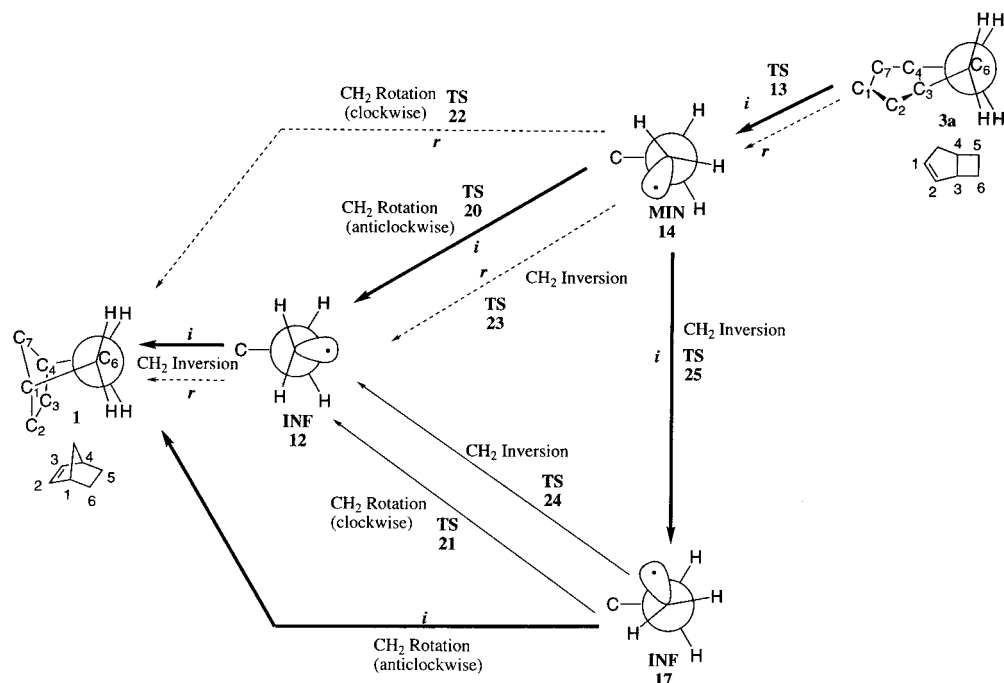
**Table 2.** Energies along the [1,3]-Sigmatropic Shift Pathway at the UB3LYP/6-31G* and CASSCF(8,8)/6-31G* Levels

structure	E_{rel} (kcal/mol)[a]	
	UB3LYP/6-31G*[b]	CAS(8,8)/6-31G*
norbornene (**1**)	0.0	0.0
bicyclo[3.2.0]hept-2-ene (**2**)	5.4	9.5
closure TS to form **2** (**13**)	50.5	54.0
gauche-in biradical (twisted 120° clockwise) (**14**)	48.3[c]	53.6
anti biradical (twisted 120° clockwise) (**15**)	–	53.1
gauche-out biradical (twisted 120° clockwise) (**16**)	–	53.4
gauche-in biradical (twisted 120° anticlockwise) (**17**)	–	53.1[c]
anti biradical (twisted 120° anticlockwise) (**18**)	–	53.4
gauche-out biradical (twisted 120° anticlockwise) (**19**)	–	53.2
TS for CH$_2$ rotation from **14** to **12** (**20**)	–	54.0[d]
TS for CH$_2$ rotation from **17** to **12** (**21**)	–	54.7[d]
TS for CH$_2$ rotation from **14** to **1** (22)	–	54.8[d]
TS for CH$_2$ inversion from **14** to **11** (23)	49.2	54.5
TS for CH$_2$ inversion from **17** to 12 (24)	–	53.8[c]
TS for CH$_2$ inversion from **14** to 17 (25)	–	53.7

[a] Energy relative to norbornene. [b] Energy includes ZPE correction. [c] Forces converged, but displacements not converged. [d] Value taken from constrained optimization.

breakage was located 45.1 kcal/mol (44.5 kcal/mol) above the product. Intrinsic reaction coordinate calculations from this transition state at the UB3LYP level led to bicyclo[3.2.0]hept-2-ene in one direction and to a very flat region corresponding to a twisted biradical in the other. No twisted biradical intermediate minimum could be fully optimized on the flat surface at the UB3LYP level in this region; the best point optimized was 2.2 kcal/mol below the transition state. At the

CASSCF/6-31G* level, we were able to optimize this *gauche-in* intermediate **14**, where the methylene is twisted by 120° clockwise, relative to structure **12**. This structure lies very close to transition state **13** for formation (or cleavage) of the C3–C6 bond; structure **14** is only 0.4 kcal/mol lower in energy than **13**. The biradical **14** can undergo torsion around the C4–C5 bond to form the similarly twisted *anti* and *gauche-out* biradicals, **15** and **16** (Figure 7). Both of these are higher energy conformers of biradicals **7** and **10**, respectively.

A second twisted *gauche-in* biradical, **17**, with a 120° anticlockwise methylene twist relative to structure **12**, was also investigated at the CASSCF level (Figure 8). As with structure
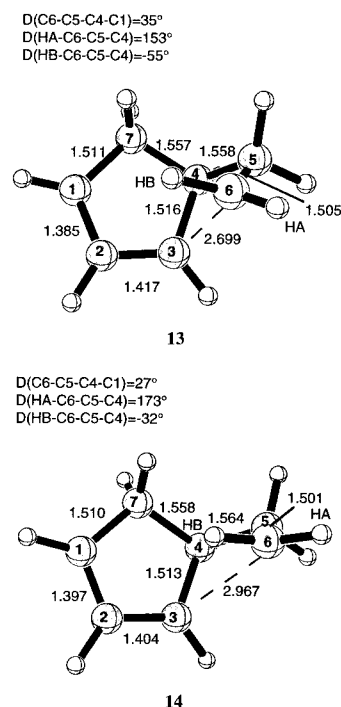
Figure 6. CASSCF/6-31G*-optimized geometries of the transition state leading to bicyclo[3.2.0]hept-2-ene **13** and the twisted *gauche-in* biradical (methylene twisted by 120° clockwise) **14**.
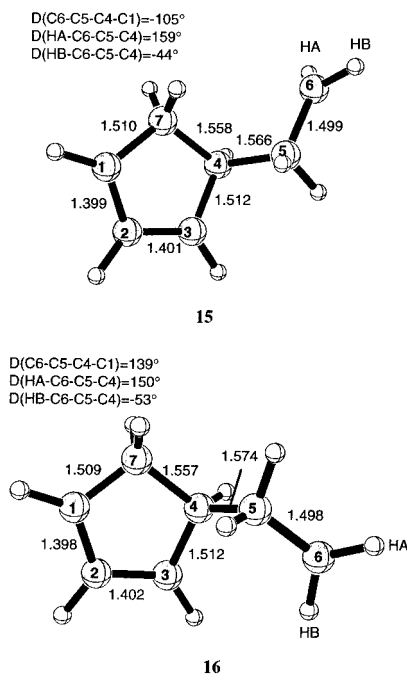
Figure 7. CASSCF/6-31G*-optimized geometries of the twisted *anti* biradical (methylene twisted by 120° clockwise) **15** and the twisted *gauche-out* biradical (methylene twisted by 120° clockwise) **16**.

12, this species is unstable with respect to closure to norbornene and could not be fully optimized (the forces converged, but the displacements did not converge). A series of constrained optimizations showed that there is no barrier for closure of this species to norbornene. Rotation about the C4–C5 bond would give the stable *anti* and *gauche-out* biradicals, **18** and **19**, where the methylene groups are similarly twisted by 120° anticlockwise.

The three conformers of the *gauche-in* biradical species (**12**, **14**, and **17**) are connected by six possible transition structures, as shown in Scheme 5. Three of the transition structures (**20**, **21**, and **22**) correspond to methylene torsions with respect to C5 and C6 maintaining CH2 pyramidalization (Figure 9). The other three (**23**, **24**, and **25**) correspond to methylene inversions (Figure 10); these involve motion of one CH bond while the other remains essentially stationary. A [1,3]-sigmatropic shift reaction path with inversion of stereochemistry must involve both a 180° methylene rotation and a methylene inversion. In Scheme 5, two possible pathways (labeled *i*) leading from the twisted biradical **14** to norbornene are marked with bold arrows: the first involves a methylene torsion through transition state **20** to form the metastable biradical **12**, followed by barrierless inversion of the methylene group to form norbornene;

the second involves initial methylene inversion through transition state **25** to form the biradical **17**, followed by a barrierless methylene torsion to form norbornene. A [1,3]-sigmatropic shift reaction path with retention of stereochemistry can involve either a methylene torsion through transition state **22** or inversion through transition state **23** to form **12**, which closes with no barrier to norbornene. These two pathways are indicated by dotted arrows and labeled *r* in Scheme 5.

Although these six transition states are formally possible, in practice the surfaces are so flat in this region that only two transition states could be fully optimized. These correspond to the two methylene inversion transition states **25** and **23** (Figure 10). The three transition states corresponding to methylene torsions (**20**, **21**, and **22**) were partially optimized by constraining the HA–C6–C5–HB torsional angles to be −160°. On relaxing the constraints, transition state **20** led to transition state **25**, while both **21** and **22** led to transition state **23**. The energies of **25** and **23** are 53.7 and 54.5 kcal/mol, respectively, which makes transition state **13** the barrier for the reaction with inversion of stereochemistry and transition state **23** the barrier for the reaction with retention of stereochemistry. Transition state **23** was also located at the UB3LYP level and found to lie 49.2 kcal/mol above norbornene, 1.3 kcal/mol below transition state **13**. The third inversion transition state, **24**, could not be fully optimized (the maximum displacements did not converge). The best structure optimized in this region is shown in Figure 10.

In Carpenter's dynamics studies, a clockwise methylene rotation led directly to bicyclo[3.2.0]hept-2-ene, whereas an anticlockwise rotation led to a more stable *anti* biradical (corresponding to structure **18**).[8] He explained the preference for stereochemical inversion of labeled substrates in terms of inertial dynamic effects which cause motions in a direction dictated by bond-breaking motions. While dynamics are undoubtedly needed to understand fully the rates of competing processes, we find that the shape of the potential surface, in particular the barriers leading from the twisted *gauche-in* biradical **14** to norbornene, are in accord with the experimentally observed stereochemistry of the products. At both levels of theory, the barrier for inversion from **14** is negligible, while the barrier for retention is about 1 kcal/mol, consistent with the small preference found experimentally for inversion.

(iii) [1,2]-Sigmatropic Shift of Norbornene To Form Tricyclo[3.2.1.0³,⁷]heptane. Norbornene can undergo a third rearrangement, a [1,2]-sigmatropic shift, leading to tricyclo-[3.2.1.0³,⁷]heptane, **4a** (Figure 1), which lies 17.9 kcal/mol (28.5 kcal/mol) above norbornene (see Table 3). The reaction is formally a [$_\pi2 + _\sigma2$] pericyclic rearrangement, which has been studied extensively by Zimmerman and others, both experi-
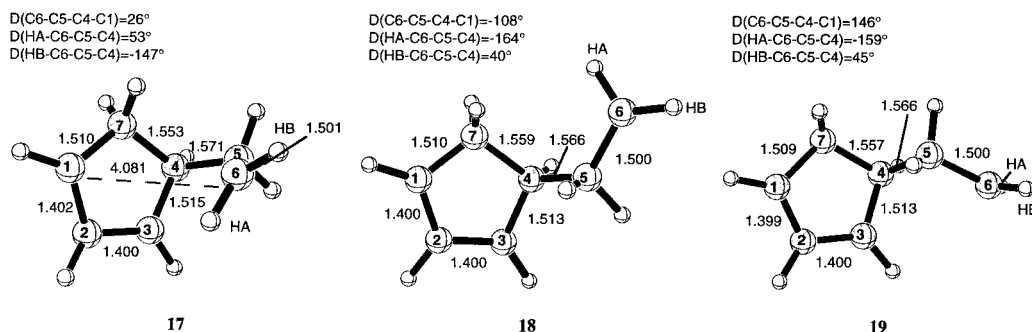
Figure 8. CASSCF/6-31G*-optimized geometries of the metastable twisted *gauche-in* biradical (methylene twisted by 120° anticlockwise) **17** (displacements not converged), the twisted *anti* biradical (methylene twisted by 120° anticlockwise) **18**, and the twisted *gauche-out* biradical (methylene twisted by 120° anticlockwise) **19**.
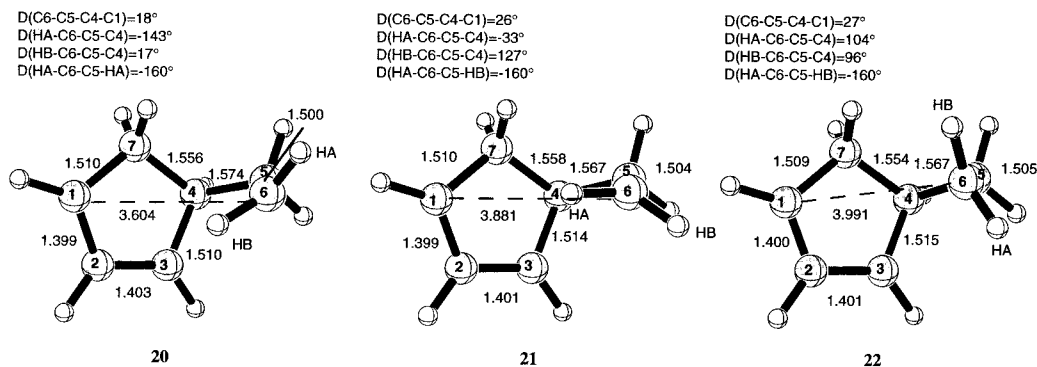
Figure 9. CASSCF/6-31G*-optimized geometries of the transition state for forming the twisted biradical (methylene twisted by 120° clockwise) from norbornene **20** (HA−C6−C5−HB torsion constrained), the transition state for forming the twisted biradical (methylene twisted by 120° anticlockwise) from norbornene **21** (HA−C6−C5−HB torsion constrained), and the transition state between the two twisted *gauche-in* biradicals **22** (HA−C6−C5−HB torsion constrained).
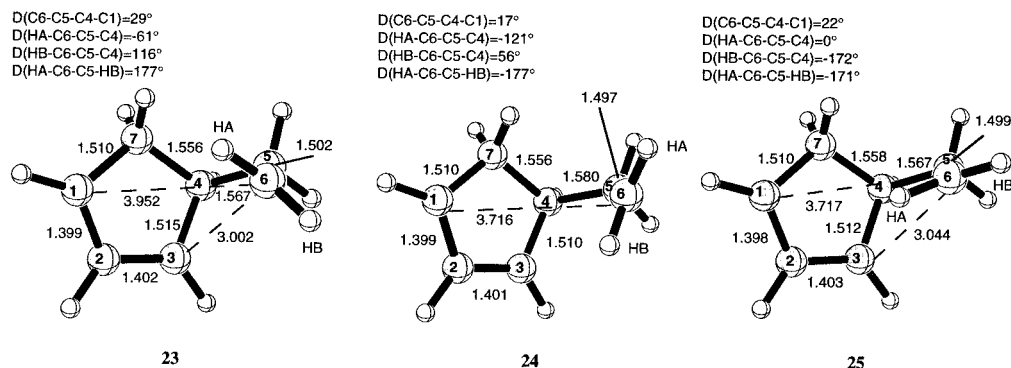
Figure 10. CASSCF/6-31G*-optimized geometries of the transition state for CH₂ inversion from the *gauche-in* biradical to the twisted *gauche-in* biradical (methylene twisted by 120° clockwise) **23**, the transition state for CH₂ inversion from the *gauche-in* biradical to the twisted *gauche-in* biradical (methylene twisted by 120° anticlockwise) **24**, and the transition state for CH₂ inversion from the twisted *gauche-in* biradical (methylene twisted by 120° clockwise) to the twisted *gauche-in* biradical (methylene twisted by 120° anticlockwise) **25**.

Table 3. Energies along the [1,2]-Sigmatropic Shift Pathway at the UB3LYP/6-31G* and CASSCF(8,8)/6-31G* Levels

structure	E_{rel} (kcal/mol)[a]	
	UB3LYP/6-31G*[b]	CAS(8,8)/6-31G*
norbornene (**1**)	0.0	0.0
tricyclo[3.2.0³,⁷]heptane (**4a**)	17.9	28.5
TS for C2−C6 bond formation (**26**)	79.8	94.3
metastable 1,3-biradical with H's up (**27**)	−	67.0[c]
metastable 1,3-biradical with H's down (**28**)	−	59.6[c]

[a] Energy relative to norbornene. [b] Energy includes ZPE correction. [c] Value taken from constrained optimization.

mentally and theoretically.[28] The reaction path is much higher in energy than either the retro Diels−Alder reaction or the [1,3]-sigmatropic shift, and therefore the [1,2]-sigmatropic shift is unlikely to occur from the ground-state surface. However, as shown in the next section, it can be accessed from the excited-state surface, and we summarize the important features of the pathway here.

The [1,2]-sigmatropic shift of norbornene to form **4a** involves cleavage of the C1−C6 bond, followed by formation of a bond between C2 and C6. As described in section (i), there is no transition state for simply stretching the C1−C6 bond. Instead, the reaction path is expected to proceed through the metastable *gauche-in* biradical, **12**. A transition state **26** (Figure 11) for formation of the C2−C6 bond from **12** was optimized and found

(28) Zimmerman, H. E.; Armestor, D. *Chem. Rev.* **1996**, *96*, 3065 and references therein.

to lie some 79.8 kcal/mol (94.3 kcal/mol) above norbornene. The 1,3-biradical formed is unstable with respect to C1−C3 bond formation and closes to form **4a** with no barrier.

A series of constrained optimizations (constraining the C1−C3 distance to be between 1.6 and 2.4 Å) indicated that two different conformations exist for the 1,3-biradical (see Scheme 6). The opening of the cyclopropane ring in **4a** is almost a pure C−C stretch, such that early in bond-breaking the two radical centers point toward each other. However, at C1−C3 distances greater than 1.9 Å, this is not the lowest energy conformation, and the radical centers invert. At 2.4 and 2.3 Å, both conformers were located; structures **27** and **28** are the two conformers obtained at 2.3 Å. The energy computed at several points between **27** and **28** showed that there is no barrier between the two conformations once the C2−C6 bond has formed, and ring-closure to form **4a** will occur very rapidly.

(iv) Cleavage of the C4−C7 (or C1−C7) Bond and [1,3]-Sigmatropic Shift To Form Bicyclo[4.1.0]hept-2-ene. The fourth isomer of norbornene considered was bicyclo[4.1.0]hept-2-ene, **3a**, the product of a [1,3]-sigmatropic shift involving initial cleavage of the C4−C7 bond. This type of species is formed both on direct photolysis of 2-cyanonorbornene and on solution photolysis of 2-trifluoromethylnorbornene.

A transition state **29** (Figure 12) for cleaving the methylene bridge (C4−C7 bond) in norbornene was located with a long breaking C4−C7 bond length (2.83 Å). This transition state lies 54.6 kcal/mol (Table 4) above norbornene and is energetically very similar to the transition state **13** for the [1,3]-sigmatropic shift leading to **2**. IRC calculations from transition state **29** led to norbornene in one direction and to an extremely flat biradical
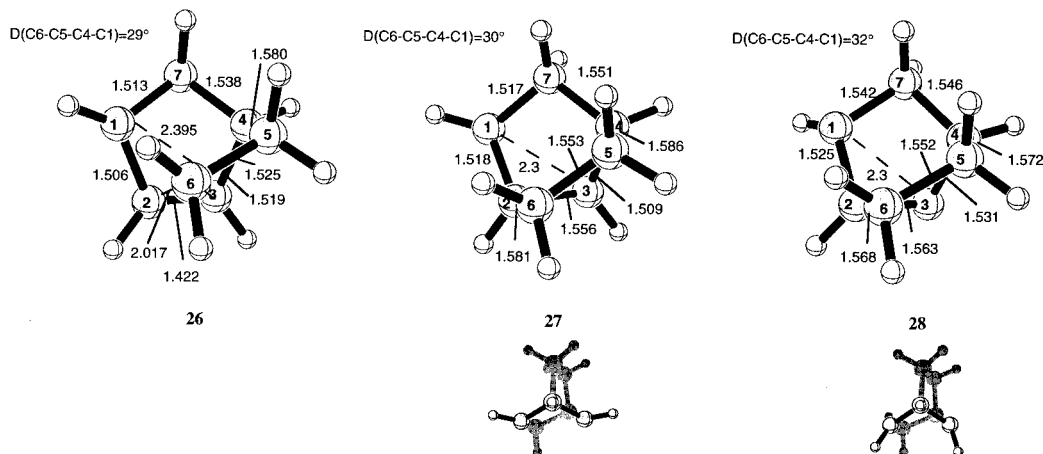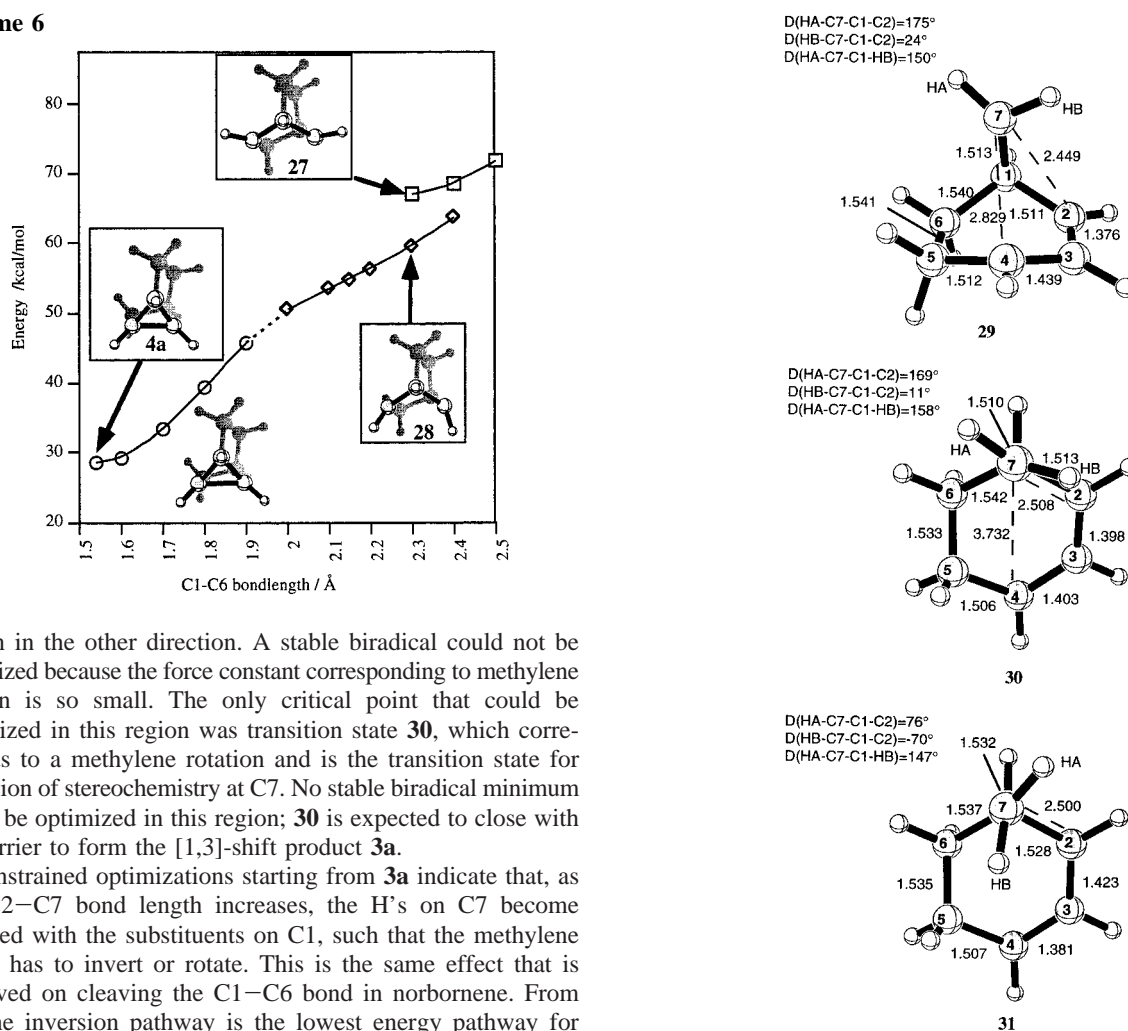
Figure 11. CASSCF/6-31G*-optimized geometries of the transition state leading to tricyclo[3.2.1.0^{3,7}]heptane **26**, the metastable 1,3-biradical with H's flipped up **27** (C1−C3 bond length constrained), and the metastable 1,3-biradical with H's flipped down **28** (C1−C3 bond length constrained).

Scheme 6

region in the other direction. A stable biradical could not be optimized because the force constant corresponding to methylene torsion is so small. The only critical point that could be optimized in this region was transition state **30**, which corresponds to a methylene rotation and is the transition state for inversion of stereochemistry at C7. No stable biradical minimum could be optimized in this region; **30** is expected to close with no barrier to form the [1,3]-shift product **3a**.

Constrained optimizations starting from **3a** indicate that, as the C2−C7 bond length increases, the H's on C7 become eclipsed with the substituents on C1, such that the methylene group has to invert or rotate. This is the same effect that is observed on cleaving the C1−C6 bond in norbornene. From **3a**, the inversion pathway is the lowest energy pathway for cleaving the C2−C7 bond; structure **31** was obtained at a constrained C2−C7 bond length of 2.5 Å with the methylene group inverted. This reaction path is analogous to the one shown in Scheme 4. Neither rotation clockwise nor anticlockwise gave rise to stable biradicals.

The [1,3]-shift of bicyclo[4.1.0]hept-2-ene is directly analogous to those of bicyclo[3.2.0]hept-2-ene and vinylcyclopropane.[29] In each case, cleaving the first bond leads to a metastable biradical region, where stereochemistry is controlled by internal

Figure 12. CASSCF/6-31G*-optimized geometries of the transition state for cleaving the methylene bridge **29**, the transition state for methylene torsion leading to inversion of stereochemistry at C7 **30**, and a metastable biradical leading to bicyclo[4.1.0]hept-2-ene **31** (C2−C7 bond length constrained).

methylene rotations which favor inversion of stereochemistry at the migrating carbon. It should also be noted that, in the transition states **13** and **29** and the vinylcyclopropane *si* transition state, there is already considerable rotation of the methylene group, which favors inversion of stereochemistry.

(29) Houk, K. N.; Nendel, M.; Wiest, O.; Storer, J. W. *J. Am. Chem. Soc.* **1997**, *119*, 10545.

Table 4. Energies of the Critical Points Located along the Pathway Corresponding to C4–C7 Bond Cleavage at the CASSCF(6,6)/6-31G* Level

structure	state	E_{rel} (kcal/mol),[a] CAS(6,6)/6-31G*
norbornene (**1**)	S_0	0.0
bicyclo[4.1.0]hept-2-ene (**3a**)	S_0	9.6
tricyclo[3.2.0^{3,7}]heptane (**4a**)	S_0	27.6
TS for cleaving methylene bridge (**29**)	S_0	54.6
TS for inversion of stereochemistry (**30**)	S_0	48.7
biradical leading to closure of **3a** (**31**)	S_0	44.2
TS for interconversion of **3a** with **4a** (**32**)	S_0	92.1
1,3-biradical with H's up (**33**)	S_0	82.5
TS for 1,3-biradical closure (**34**)	S_0	84.2
1,3-biradical with H's down (**35**)	S_0	74.0[b]

[a] Energy relative to norbornene. [b] Value taken from constrained optimization.
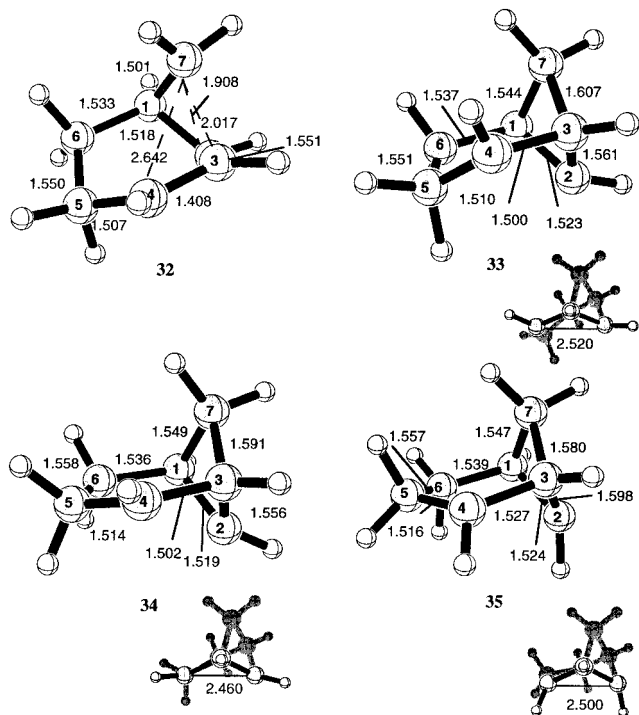
Figure 13. CASSCF/6-31G*-optimized geometries of the transition state for interconversion of tricyclo[3.2.1.0^{3,7}]heptane with bicyclo[4.1.0]-hept-2-ene **32**, the 1,3-biradical with H's flipped up **33**, the transition state for closure of 1,3-biradical **34**, and the metastable 1,3-biradical with H's flipped down **35** (C2–C4 bond length constrained).

(v) Bicyclo[4.1.0]hept-2-ene to Tricyclo[3.2.1.0^{3,7}]heptane Reaction Path. Finally we describe the ground-state reaction path for the interconversion of bicyclo[4.1.0]hept-2-ene, **3a**, with tricyclo[3.2.1.0^{3,7}]heptane, **4a**, another formal [$_\pi 2 + _\sigma 2$] process. As with the [1,2]-sigmatropic shift of norbornene involving cleavage of the C1–C6 bond, this process is strongly disfavored. Structure **32** is the transition state for the [1,2]-shift of bicyclo-[4.1.0]hept-2-ene, **3a** (Figure 13), and lies 92.1 kcal/mol above norbornene (Table 4); IRC calculations from this transition state led to **3a** in one direction and to the 1,3-biradical **33** in the other. This 1,3-biradical is analogous to structure **27**, where the H's are facing up and the methylene centers are pointing toward each other. However, unlike **27**, **33** is a stable 1,3-biradical, and there is a small barrier (1.7 kcal/mol) corresponding to transition state **34** for ring-closure to form **4a**. This barrier involves a change in the conformation of the original six-membered ring (i.e., the C4–C5–C6 unit flips up), coupled with flipping the H's down. There is no stable 1,3-biradical with

Table 5. Energies of Critical Points Located along the $^1(\pi\pi^*)$ Retro Diels–Alder Reaction Paths at the CAS(8,8)/6-31G* Level

structure	state	E_{rel}(kcal/mol),[a] CAS(8,8)/6-31G*
norbornene (**1**)	S_0	0.0
	$^1(\pi\pi^*)$	205.5[b]
	$^1(\sigma\pi^*)$	241.3
$^1(\pi\pi^*)$ cyclopentadiene + ethylene	$^1(\pi\pi^*)$	138.2[c]
S_1/S_0 conical intersection (**36**)	$^1(\pi\pi^*)$	104.7
	S_0	104.7
second-order saddle point (**38**)	$^1(\pi\pi^*)$	188.1
SOSP for cleaving C1–C6 bond (**39**)	$^1(\pi\pi^*)$	193.5[d]
TS leading to anti biradical (**40**)	$^1(\pi\pi^*)$	135.3
anti biradical (**41**)	$^1(\pi\pi^*)$	125.5
TS leading to *gauche-out* biradical (**42**)	$^1(\pi\pi^*)$	135.8
gauche-out biradical (**43**)	$^1(\pi\pi^*)$	125.5
gauche-in biradical (**44**)	$^1(\pi\pi^*)$	126.4
TS between **44** and conical intersection **36** (**45**)	$^1(\pi\pi^*)$	126.9
TS between **41** and **44** (**46**)	$^1(\pi\pi^*)$	131.0
TS between **43** and **44** (**47**)	$^1(\pi\pi^*)$	130.2

[a] Energy relative to norbornene. [b] This energy is corrected to 163.7 kcal/mol using CASPT2N calculations. [c] Constrained to have C_{2v} symmetry. [d] Forces converged, but displacements not converged.

Table 6. Energies of the Critical Points Located along the Excited-State Pathway Corresponding to C4–C7 Bond Cleavage at the CASSCF(6,6)/6-31G* Level

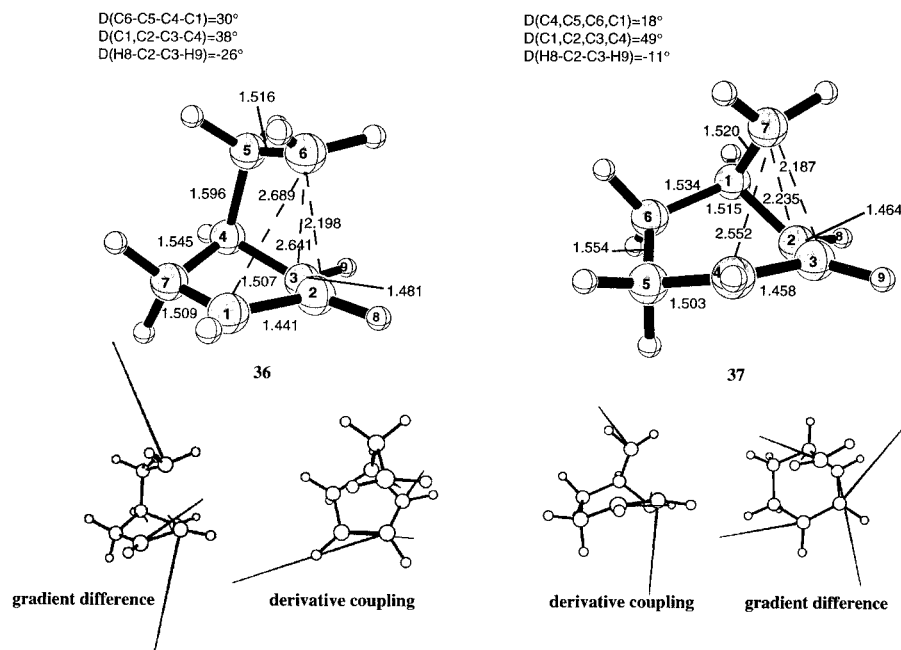| structure	state	E_{rel} (kcal/mol)[a] CAS(6,6)/6-31G*
norbornene (**1**)	S_0	0.0
	$^1(\pi\pi^*)$	205.7
S_1/S_0 conical intersection (**37**)	$^1(\pi\pi^*)$	113.1
	S_0	113.1
second-order saddle point (**38**)	$^1(\pi\pi^*)$	188.2
SOSP for cleaving methylene bridge (**48**)	$^1(\pi\pi^*)$	191.4[b]
S_1/S_0 conical intersection (**49**)	$^1(\pi\pi^*)$	114.2
	S_0	114.2

[a] Energy relative to norbornene. [b] Single point at CAS(4,4)/6-31G*-optimized geometry.

H's flipped down. Structure **35** was optimized with the C1–C3 distance constrained to be 2.5 Å.

Excited-State Surface. In this section we describe the nature of the critical points located on the $^1(\pi\pi^*)$ surface of norbornene. The structures optimized at the CASSCF/6-31G* level are shown in Figures 14–18, with the corresponding energies in Tables 5 and 6. The focal points of the potential energy surface are the two conical intersections, **36** and **37** (Figure 14), that efficiently funnel molecules from the $^1(\pi\pi^*)$-state to the ground-state surface. These funnels, which are accessed via small barriers once the $^1(\pi\pi^*)$ surface is populated, also determine the reaction path taken on the ground-state surface. In this section, we describe possible excited-state reaction paths that lead to these conical intersections.

The $^1(\pi\pi^*)$ surface is calculated to lie some 206 kcal/mol above the ground-state surface at the CAS(8,8)/6-31G* optimized reactant geometry **1**. This value drops to 163.7 kcal/mol after correction using CASPT2N calculations. The experimental vertical excitation energy of norbornene is 146 kcal/mol (6.34 eV), well below the 184 kcal/mol (8.0 eV) available in the Zewail experiments. Experiments at 137 kcal/mol produce similar results, even though the energy is below that of the vertical $\pi\pi^*$ state. This is most probably due to rapid internal conversion from the Rydberg state to the descending $\pi\pi^*$ state before the conical intersection regions.

On the $^1(\pi\pi^*)$ surface, norbornene initially undergoes a C2–C3 bond stretch. A second-order saddle point (SOSP), **38** (Figure

D(C6-C5-C4-C1)=30°
D(C1,C2-C3-C4)=38°
D(H8-C2-C3-H9)=-26°

D(C4,C5,C6,C1)=18°
D(C1,C2,C3,C4)=49°
D(H8-C2-C3-H9)=-11°

36

37

gradient difference   derivative coupling   derivative coupling   gradient difference

Figure 14. CASSCF/6-31G*-optimized geometries of the $^1(\pi\pi^*)$/S_0 conical intersections **36** and **37**, with derivative coupling and gradient difference vectors shown below.

15), was located at a C2−C3 bond length of 1.55 Å, 17.4 kcal/mol below the vertical excitation energy. Further C2−C3 stretching leads to a crossing of the $^1(\pi\pi^*)$ and $^1(\sigma\pi^*)$ surfaces. At the SOSP, the ethylene group is still planar, and this structure is analogous to the planar transition structure for rotation about the C−C bond in triplet ethylene. The p orbitals of the two carbons prefer to be orthogonal. In the case of $^1(\pi\pi^*)$ norbornene, the geometry is constrained by the ring, and therefore the ethylene carbons pyramidalize to minimize the π orbital overlap. The two negative directions of curvature at the SOSP correspond to pyramidalization in a symmetric motion, retaining C_s symmetry, either upward or downward, or to pyramidalization in an antisymmetric motion where H8 and H9 move in opposite directions. This was confirmed by computing the vibrational frequencies in a reduced active space without the σ orbitals in the C−C bonds that are broken. The lowest positive vibrational frequency (170 cm^{-1}) at the SOSP corresponds to a C6−C5−C4−C1 twist coupled with a C1−C2−C3−C4 torsion, and this is the motion required to access the conical intersections. It is clear that there should be lower energy pyramidalized minima, but most likely due to crossing of the $^1(\pi\pi^*)$ state with the $^1(\sigma\pi^*)$ states, we were unable to optimize any minima in this region.

Several different pathways are possible from this SOSP or the corresponding lower energy pyramidal species: (i) a stepwise retro Diels−Alder path involving one-bond (C1−C6) cleavage; (ii) a concerted retro Diels−Alder pathway involving simultaneous two-bond (C1−C6 and C4−C5) cleavage; and (iii) a pathway involving cleavage of the C4−C7 bond. In this section we will consider each of these reaction paths in turn.

(i) Excited-State Stepwise Retro-Diels−Alder and Diels−Alder Pathways. Structure **39** (Figure 15) was located, although not fully optimized (maximum displacements did not converge), corresponding to C1−C6 bond cleavage from the SOSP **38**. A lower energy structure for cleaving the C1−C6 bond could not be optimized. However, structure **39** provides an upper bound to the energy required to access the conical intersection, which is only 5 kcal/mol above the SOSP **38** and 12 kcal/mol below the computed vertical excitation energy. A frequency calculation,

carried out with a reduced active space of four electrons in four orbitals, showed three negative directions of curvature. The first imaginary frequency corresponds to C1−C6 bond cleavage coupled with a decrease in the C2−C3 bond. The second and third imaginary frequencies correspond to pyramidalization of C3 and C2, respectively.

Once the C1−C6 bond cleaves, rotation about the C4−C5 bond takes place, and there is a change in the way the electrons are coupled. As the C5−C6 fragment rotates across the face of the ring, the electrons on C1 and C6 decouple, and the electron on C6 couples with that on C2. This has the effect of stabilizing the excited-state surface as the two unpaired electrons are on C1 and C3 instead of being on adjacent carbons. It also destabilizes the ground-state surface in this arrangement as only two electrons are coupled, instead of the preferred four. This leads to a rapid decrease in the energy gap between the two surfaces which eventually cross. The lowest energy point optimized where the two surfaces cross is the conical intersection **36** (Figure 14).

We also located the structures involved in the stepwise Diels−Alder addition of the excited S_1 state (2^1A_1) of cyclopentadiene to ethylene (Figures 16 and 17). The minimum corresponding to the 2^1A_1 state of cyclopentadiene could not be fully optimized. Kovar and Lischka previously optimized an excited 2^1A_1 cyclopentadiene structure with C_{2v} symmetry using MC-SCF calculations which lies 127 kcal/mol above the ground state of cyclopentadiene.[30] A frequency calculation at this geometry indicated three imaginary frequencies corresponding to out-of-plane motions, but they could not optimize a minimum as the surface was so flat along these coordinates. We optimized a similar structure which lies 138.2 kcal/mol about the ground state of norbornene at the CASSCF(8,8)/6-31G* level.

The reaction of this excited-state cyclopentadiene with ethylene can go through an *anti* transition structure **40** to give an *anti* biradical **41**, or a *gauche-out* transition structure **42** to give a *gauche-out* biradical **43** (Figure 16). Both of these pathways have almost no barrier. The reaction proceeds in a

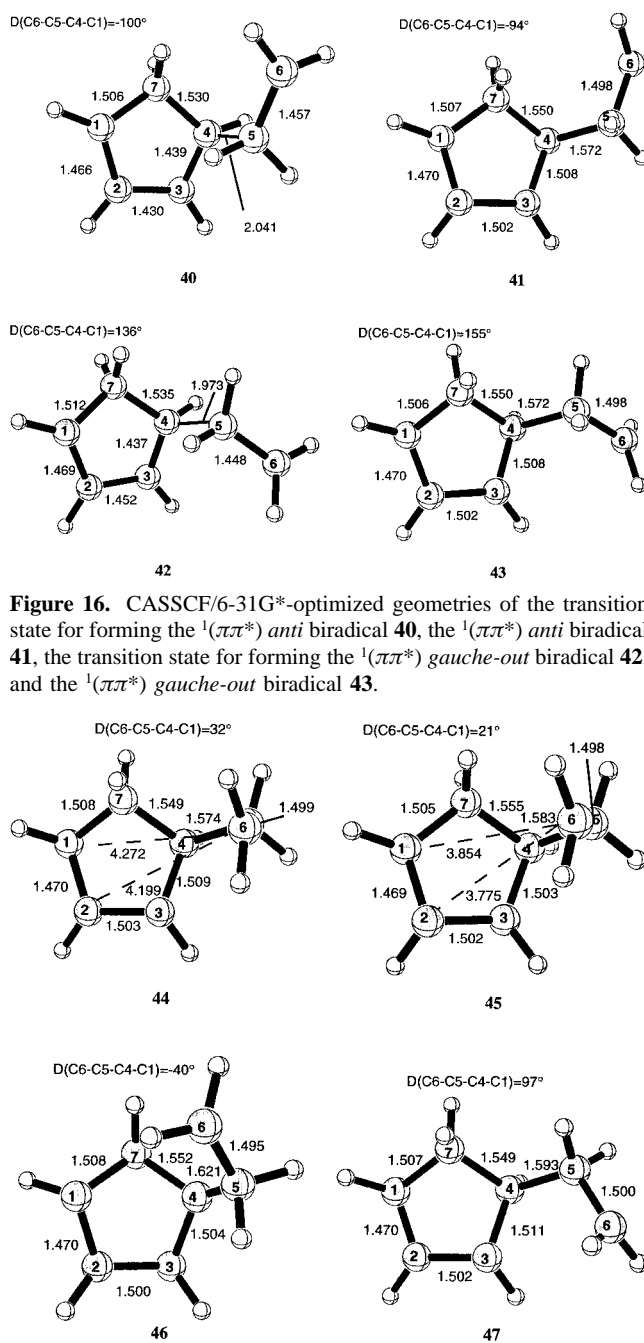(30) Kovár, T.; Lischka, H. *J. Mol. Struct. (THEOCHEM)* **1994**, *303*, 71.
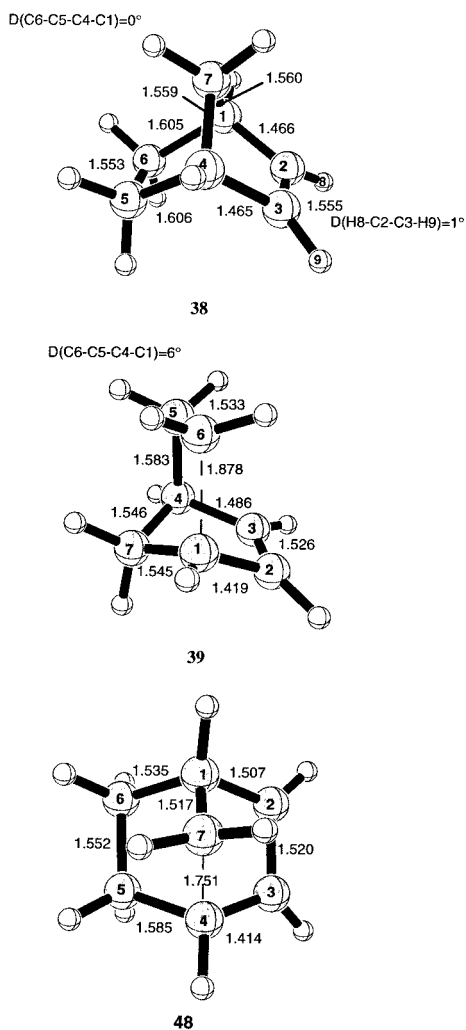
Figure 15. CASSCF/6-31G*-optimized geometries of the $^1(\pi\pi^*)$ second-order saddle point close to norbornene **38**, the third-order saddle point corresponding to C1−C6 bond cleavage **39**, and the second-order saddle point corresponding to C4−C7 bond cleavage **48** (displacements not converged).


Figure 16. CASSCF/6-31G*-optimized geometries of the transition state for forming the $^1(\pi\pi^*)$ *anti* biradical **40**, the $^1(\pi\pi^*)$ *anti* biradical **41**, the transition state for forming the $^1(\pi\pi^*)$ *gauche-out* biradical **42**, and the $^1(\pi\pi^*)$ *gauche-out* biradical **43**.

Figure 17. CASSCF/6-31G*-optimized geometries of the $^1(\pi\pi^*)$ *gauche-in* biradical **44**, the transition state leading from the $^1(\pi\pi^*)$ *gauche-in* biradical to the conical intersection **45**, the $^1(\pi\pi^*)$ *anti/gauche-in* transition state **46**, and the $^1(\pi\pi^*)$ *gauche-out/gauche-in* transition state **47**.

fashion similar to the ground-state stepwise process; however, on the excited-state surface, the *gauche-in* intermediate **44** (Figure 17) corresponds to a stable structure that could be fully optimized. This species lies close to the conical intersection **36** in geometry but some 22 kcal/mol higher in energy. The barrier corresponding to transition structure **45** separating the *gauche-in* biradical from the conical intersection is only 0.5 kcal/mol. Therefore, **44** should decay to the ground-state surface very efficiently. Barriers corresponding to the transition structures **46** and **47** connecting the *gauche-in* biradical **44** to the *anti* and *gauche-out* biradicals were also found. All of these barriers are low and might disappear with the inclusion of dynamic correlation.

Therefore, both the excited-state retro Diels−Alder reaction and the excited-state Diels−Alder reaction proceed through the same conical intersection, **36**, and are thus expected to give similar products on the ground-state surface. However, the distribution of products on the ground-state surface is expected to vary according to the angle at which decay through the intersection occurs, and this angle may be influenced by the direction from which the conical intersection is approached on the excited state.[10]

(ii) Excited-State Concerted Retro Diels−Alder Pathway. The excited-state concerted retro Diels−Alder pathway was examined by stretching both C−C bonds (C1−C6 and C4−C5) simultaneously and constraining them to be between 1.8 and 2.4 Å. The reaction profile along this symmetric bond-breaking coordinate is shown in Scheme 7. The energies of these points are much higher than for the analogous stepwise geometries, in accordance with expectation.[9] These results indicate that the excited-state concerted pathway lies considerably higher in energy than the stepwise pathways, with a barrier of at least 30 kcal/mol leading to it. This barrier could not be optimized but appears to occur at around 1.75 Å. There were problems with converging symmetric geometries at bond lengths less than this.

Scheme 7
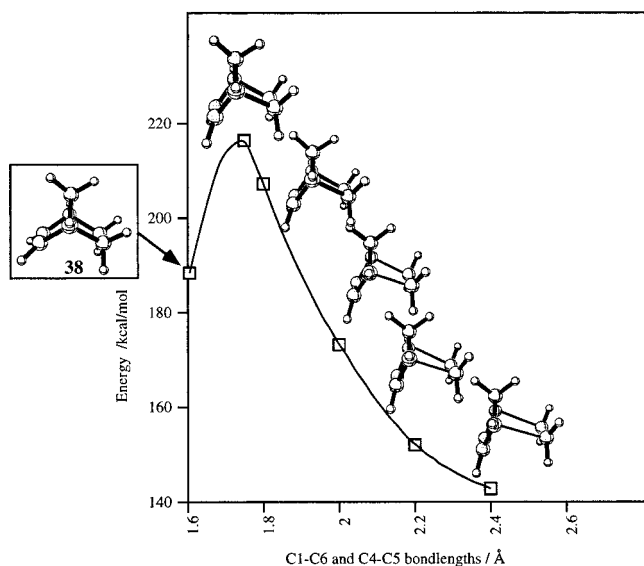
(iii) Excited-State Pathway for Cleaving the C4−C7 Bond. A structure corresponding to C4−C7 bond cleavage from **38** could not be fully optimized in a (6,6) active space. A SOSP **48** corresponding to C4−C7 bond cleavage was optimized in a (4,4) active space without the C2−C3 σ and σ^* orbitals (Figure 15). A single point in the large active space placed this barrier 3 kcal/mol above **38** and 14 kcal/mol below the vertical excitation energy. Calculation of the vibrational frequencies showed two imaginary frequencies: the first imaginary frequency corresponds to C4−C7 bond cleavage coupled strongly with a symmetric pyramidalization motion of C2 and C3, while the second imaginary frequency corresponds to C4−C7 bond cleavage coupled to antisymmetric pyramidalization of C2 and C3.

A series of SOSPs were optimized, starting from **38** and constraining the C4−C7 distance. These showed a steady increase in energy up to a C4−C7 distance of 2.0 Å, when the energy reaches 203.2 kcal/mol, only 2.3 kcal/mol below the vertical excitation energy. At distances greater than 2.0 Å, a rapid drop in energy is observed with a change in the coupling of the electrons from C4−C7 to C3−C7. No lower energy structure could be optimized corresponding to C4−C7 bond cleavage, but this structure can be thought of as an upper bound to the energy for this process. In fact, the surface is populated from such a high energy in the femtosecond laser experiments that any barrier on the excited-state surface is expected to be irrelevant.

As with the excited-state stepwise retro Diels−Alder reaction, bond cleavage is followed by rotation over the ring to bring C3 and C7 closer together. This leads to a change in the coupling of the electrons on the excited state, which simultaneously stabilizes S_1 and destabilizes S_0, leading to the second conical intersection region. Two different conical intersections were located in this region. Structure **37** (Figure 14) is the lowest energy structure on the conical intersection hyperline, and this is the one we shall discuss in detail in the next section. However, a third conical intersection (**49**) was also located on this hyperline, only 1 kcal/mol higher in energy. It differs in structure from **38** mainly in the conformation of the six-membered ring (Figure 18). These results indicate that the degeneracy spans many different geometries with a range of H8−C2−C3−C9 torsional angles and six-membered ring conformations. In practice, decay can occur at any of these geometries, and in the
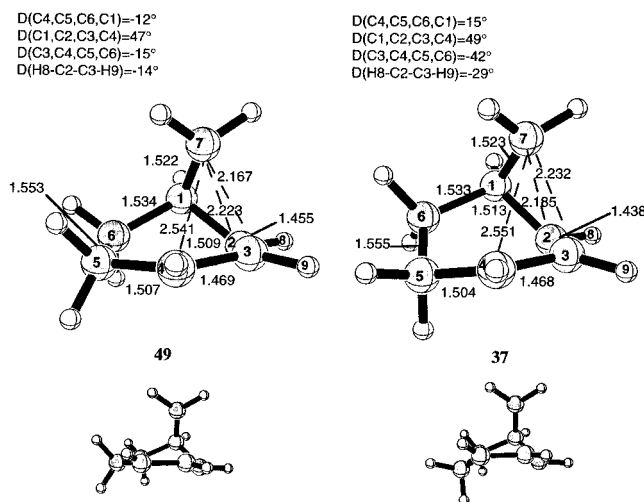

Figure 18. CASSCF/6-31G*-optimized geometries of the conical intersections **49** and **37**.

Scheme 8

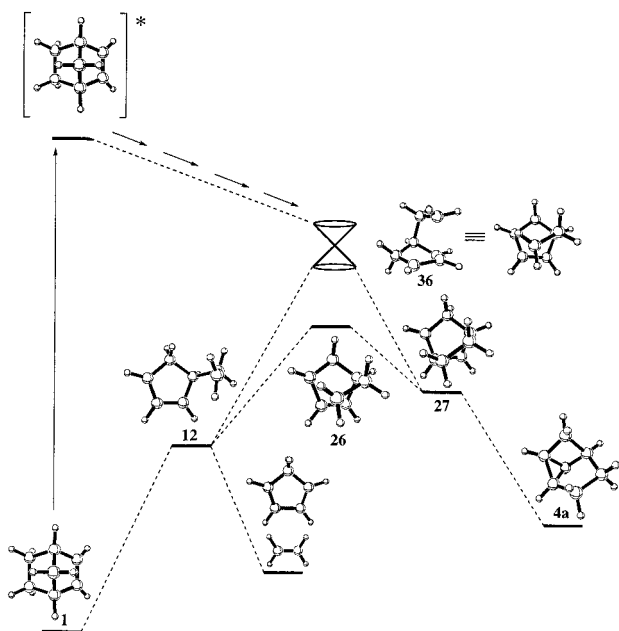next section we will discuss how this may also affect the lifetimes of species on the ground-state surface.

Conical Intersection Regions. As mentioned in the previous sections, the conical intersection regions are accessed after cleavage of a single C−C bond (either C1−C6 or C4−C7). Structures **36** and **37** (or **49**) are geometrically very similar, having four electrons arranged roughly in a tetrahedral array which can couple in three different ways (see Scheme 8). In the $^1(\pi\pi^*)$ state of norbornene, a coupling of the electrons on C2 with C6 (**36**) or C3 with C7 (**37**) is preferred, as this keeps the other two unpaired electrons apart, stabilizing the excited-state species. On the ground-state surface, the electrons can couple in three different ways, leading to norbornene (where the electrons coupled are on C1−C6, C2−C3 in **36** and C4−C7, C2−C3 in **37**), [1,2]-sigmatropic rearrangement product **4a** (C2−C6, C1−C3 in **36** and C3−C7, C2−C4 in **37**), or [1,3]-sigmatropic rearrangement products **2** and **3a** (C3−C6, C1−C2 in **36** and C2−C7, C3−C4 in **37**).

The gradient difference and derivative coupling vectors obtained at the conical intersections are also shown in Figure 14. Any linear combination of these vectors causes the degeneracy to be lifted, and therefore these vectors give an indication of possible reaction paths available on the ground-state surface after decay.
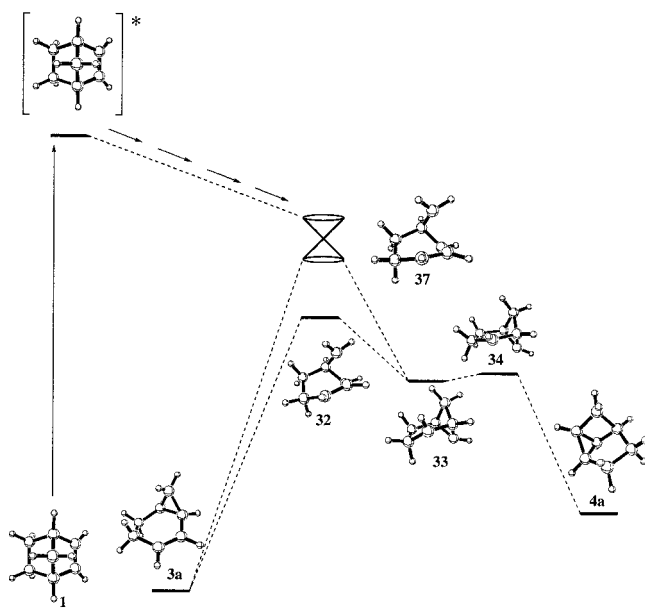
The gradient difference vector for **36** corresponds to a change in the C2−C6 bond length, while the derivative coupling vector corresponds to a concurrent change in the C2−C3 and C1−C2 bond lengths. For structure **37**, it is the derivative coupling that corresponds to a change in the C3−C7 bond length, while the gradient difference corresponds to a change in the C2−C3 and C3−C4 bond lengths. Motion in either direction along each of these vectors gives rise to many different ground-state products, which we will describe briefly. A schematic representation of the relationships between these vectors and possible reaction paths on the ground-state surface are shown in Schemes 9−12.

Following the gradient difference vector from **36** (Scheme 9) and the derivative coupling vector in **37** (Scheme 10) and decreasing the C2−C6 or C3−C7 distances leads to the
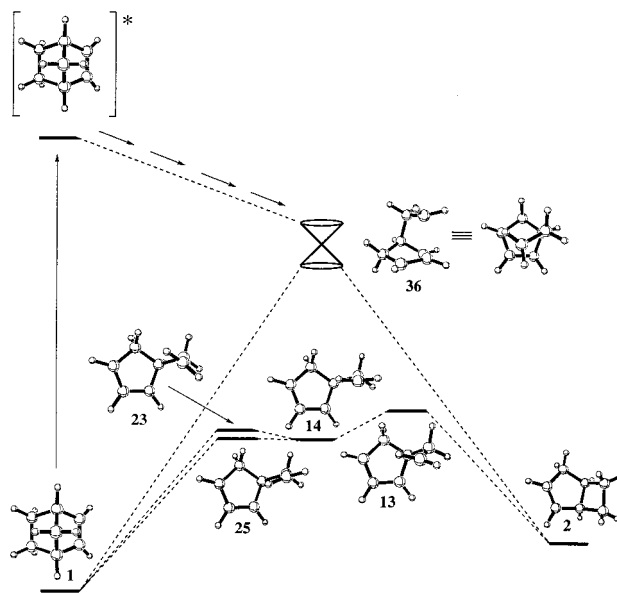
Scheme 9

Scheme 10

Scheme 11

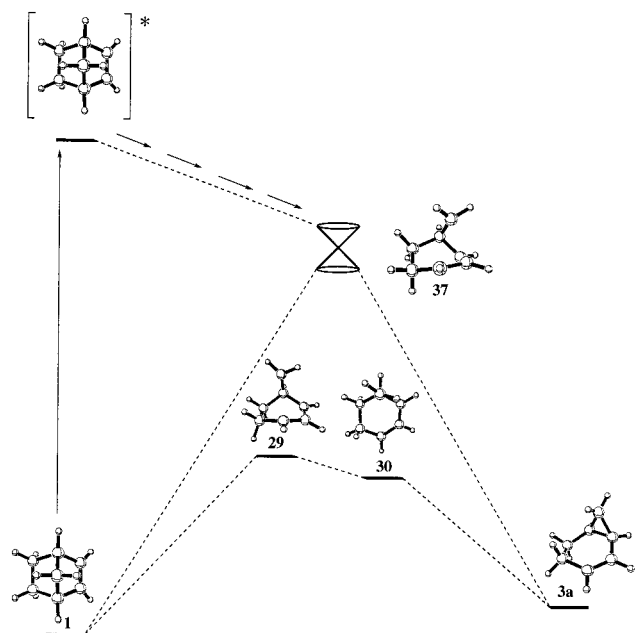and this will also affect the lifetimes of any species on the ground-state surface.

When the gradient difference vector for **36** is followed in the opposite direction, the C2−C6 distance increases, and we arrive in the *gauche-in* biradical region **12**. Many different options are available to the molecule once it is in this region of the potential surface. Closure to norbornene will occur with essentially no barrier. Alternatively, fragmentation could occur, as the biradical will have much excess energy and no means to dissipate it as the reactions are carried out in the gas phase and occur much faster than collisions. This fragmentation will lead to ethylene and cyclopentadiene, both of them highly vibrationally excited.

When the derivative coupling vector for **37** is followed in the opposite direction, the biradical region around **30** and **31** is reached. This will lead predominantly to the 1,3-sigmatropic shift product, **3a**. The structure of the conical intersection **37** suggests that, unlike the corresponding ground-state reaction path, product formation will most likely occur with retention of configuration at C7.

The derivative coupling vector in **36** (Scheme 11) and the gradient difference vector in **37** (Scheme 12) correspond to changes in the C1−C2 and C2−C3 bond lengths and the C3−C4 and C2−C3 bond lengths, respectively. A decrease in the C2−C3 bond length coupled with an increase in the C1−C2 bond length for **36**, and a decrease in the C2−C3 bond length coupled with an increase in the C3−C4 bond length for **37**, leads to norbornene in both cases. Alternatively, an increase in the C2−C3 bond length coupled with a decrease in the C1−C2 or C3−C4 bond lengths will lead to the [1,3]-sigmatropic shift products, bicyclo[3.2.0]hept-2-ene (**2**) and bicyclo[4.1.0]-hept-2-ene (**3a**), respectively. All of these ring-closures are expected to occur with no barriers as the C1−C6, C3−C6, C4−C7 and C2−C7 distances are so short at the conical intersection structures (2.7, 2.6, 2.5, and 2.2 Å respectively).

In summary, once decay through either of the conical intersections has occurred, there are many different reaction paths available on the ground-state surface. [1,2]-sigmatropic shifts, [1,3]-sigmatropic shifts, and reversion back to norbornene can all compete. In the case of conical intersection **36**, there is also the option of efficient fragmentation leading to vibrationally excited cyclopentadiene. All these routes are likely to be

formation of the 1,3 biradicals **27** and **33**, respectively. These are the two biradicals that exist along the [1,2]-sigmatropic shift reaction pathways. The ground-state transition state for formation of the C2−C6 bond (**26**) is very close in geometry to the conical intersection geometry **36**, while the ground-state transition state **32** for interconversion of **3a** and **4a** is very similar to the conical intersection geometry **37**. Both 1,3-biradicals **27** and **33** are expected to have short lifetimes before closure to the tricyclic product occurs. Biradical **27** has no barrier to ring-closure, while biradical **33** has a barrier of about 1.7 kcal/mol with CASSCF. However, as mentioned in the previous section, the conical intersection **37** spans a range of geometries with different H8−C2−C3−H9 torsional angles, such that decay could occur at a geometry closer to conical intersection **49** and arrive on the ground-state surface close to biradical **35**, in which case ring-closure will occur with no barrier. In the gas-phase experiments, the species will have a great deal of excess energy,

Scheme 12

accessible, as the molecule will have a great deal of excess energy once it has decayed through a conical intersection.

Conclusions

We have identified two regions on the potential energy surface where the $^1(\pi\pi^*)$ and ground-state surfaces cross. The first occurs at a geometry close to a *gauche-in* biradical species formed by cleavage of one allylic bond to the ethano bridge. The second conical intersection is formed after cleavage of the allylic bond to the methylene bridge. The mass 94 amu species observed in the femtosecond laser-induced decomposition could be one of several metastable biradicals formed after decay through either of the conical intersections. Compounds **2**, **3a**, and **4a** can all be formed from such a short-lived species, which only needs to complete a vibrational motion to collapse to a stable product (Scheme 13). The unstable *gauche-in* species, **12**, the biradical **31** leading to bicyclo[4.1.0]hept-2-ene, and one of the biradicals **27** and **35** leading to the highly strained tricyclic species **4a** can all be formed by only small geometric displacements from one of the conical intersection geometries, consistent with the observed instantaneous buildup of the mass 94 amu species. Each of these leads to stable ground-state products with no barrier, consistent with the exceedingly short lifetime of 160 fs.

The lifetime of the cyclopentadiene species, on the other hand, is consistent with the formation of a highly vibrationally excited species after fragmentation on the ground-state surface from the conical intersection structure **36**. The buildup time of 30 fs is the time taken for decay through the conical intersection and cleavage of the second bond to occur, while the 220 fs decay time corresponds to the time taken for the "hot" cyclopentadiene to redistribute its excess vibrational energy. The conversion of the conical intersection **36** to a *gauche-in* biradical, essentially a vibrationally excited concerted geometry on the ground-state surface, will lead to prompt cyclopentadiene formation, a retro Diels−Alder reaction.

Scheme 13
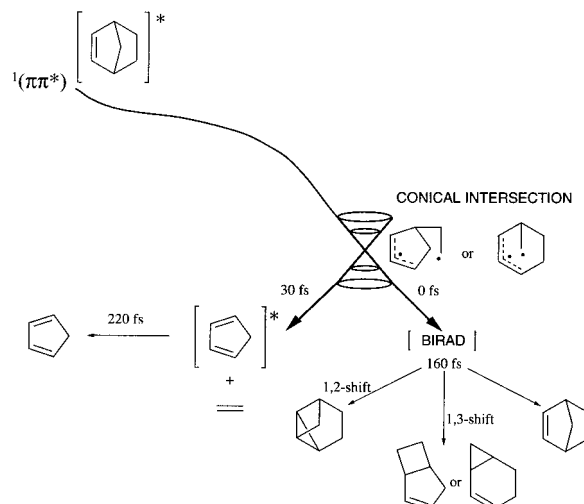
The retro Diels−Alder reaction paths on the $^1(\pi\pi^*)$ surface are very different from those on the ground-state surface. The concerted pathway is the lowest for the ground-state surface, and the two stepwise pathways (corresponding to breaking either the C1−C6 bond or the C4−C5 bond first) lie higher in energy by about 12 kcal/mol. The extent of stepwise reaction is much smaller under normal thermolysis conditions. The ground-state stepwise path involves rotation about the C4−C5 bond, a process while should take picoseconds, and produces intermediates bound by 5 kcal/mol.[4] Conversion of these to products would be slow in a thermally equilibrated case.

In contrast, on the $^1(\pi\pi^*)$ surface, the stepwise pathways are lower in energy than the concerted, with the concerted pathway forming a ridge between the stepwise paths. This is a classic example of how population of an excited state surface can provide an efficient way of accessing reaction paths that are otherwise forbidden on the ground-state surface. In the femtosecond experiments, the complex topology of the ground-state surface is revealed, whereas most of it is never explored in the thermal experiments. Future work in this area involves direct dynamics calculations from the excited state surface to determine which of the pathways revealed by the calculations are executed by the vibrationally excited species produced in the experiments.